Front. Optoelectron. 2016, 9(3): 399–405
DOI 10.1007/s12200-016-0571-x

RESEARCH ARTICLE

Large-range tunable fractional-order differentiator based on cascaded microring resonators

Ting YANG, Shasha LIAO, Li LIU, Jianji DONG (✉)

Wuhan National Laboratory for Optoelectronics (WNLO), Huazhong University of Science and Technology, Wuhan 430074, China

Abstract In this paper, we experimentally demonstrate an all-optical continuously tunable fractional-order differentiator using on-chip cascaded electrically tuned microring resonators (MRRs). By changing the voltage applied on a MRR, the phase shift at the resonance frequency of the MRR varies, which can be used to implement tunable fractional-order differentiator. Hence fractional-order differentiator with a larger tunable range can be obtained by cascading more MRR units on a single chip. In the experiment, we applied two direct current voltage sources on two cascaded MRRs respectively, and a tunable order range of 0.57 to 2 have been demonstrated with Gaussian pulse injection, which is the largest tuning range to our knowledge.

Keywords all-optical devices, optical differentiator, optical signal processing

1 Introduction

Optical differentiation is one of the basic function building blocks to implement optical signal processors for ultra-fast computing and signal processing [1]. Optical differentiator has received significant attentions lately due to its wide applications in numerous fields such as optical computing, optical communications, optical metrology, optical digital processing and analog processing, and optical sensing [2–7].

Over the last few years, lots of methods have been proposed to implement all-optical temporal differentiation. Specially designed fiber Bragg gratings (FBGs) [8], phase-shifted FBG [3], long period fiber grating [6], interferometers [9], semiconductor optical amplifier (SOA) [10], silicon-based microring resonator (MRR) [4,11,12], Mach-Zehnder interferometer (MZI) [13] and directional coupler [14,15] have been proved to be effective approaches for integer-order differentiators. Meanwhile, silicon-based photonic integrated circuit is one of the most promising candidates due to its intrinsic advantages of compact footprint, well integration capability and compatibility with complementary metal-oxide semiconductor (CMOS) technology.

In addition, fractional-order differentiator is also useful in optical encryption, which can be considered as a generalization of integer-order differentiator [16]. A fractional-order differentiator based on a photonic MZI was proposed by Cuadrado-Laborde for the first time [16]. Later, more effective schemes and optical devices have been demonstrated, including asymmetrical phase-shifted FBG [17] and long period fiber grating [18]. But in these schemes, the tunability of the differentiation order was not mentioned. Afterwards, cascaded tilted FBGs were employed to provide a tunable fractional order from 0.81 to 1.42 [19], and a tunable fractional-order differentiator with a tuning range of 0.95 – 1.72 has been demonstrated by optically pumping a tilted FBG [20]. For silicon based devices, Shahoei et al. for the first time presented a tunable fractional-order differentiator using a silicon-on-isolator (SOI) MRR with a multimode interference (MMI) coupler. The tuning range of fractional order covered from 0.37 to 1.3 [21]. Afterward, we demonstrated tunable fractional-order differentiators based on electrically tuned MZI [22] and MRR [23], with tuning ranges of 0.83 – 1.03 and 0.58 – 0.97, respectively. And Jin et al. proposed a novel photonic fractional-order differentiator based on the inverse Raman scattering (IRS) in the side-coupled silicon MRR [24]. By controlling the power of the pump lightwave, a continuously tunable differentiation order covering from 0.3 to 1.6 was achieved. As we know, the tunability of the differentiation order is one of the important figure-of-merits in fractional-order differentiator. And a large tunable range indicates more widely applications, such as immunity to cracking of encryption operation.

Received October 30, 2015; accepted December 28, 2015

E-mail: jjdong@mail.hust.edu.cn

In this paper, we experimentally demonstrate an all-optical continuously tunable fractional-order differentiator using on-chip cascaded electrically tuned MRRs. These MRRs are designed with near-critical coupling condition to meet the differentiator requirements. By changing the voltages applied on the MRRs, the phase shifts at the resonance frequencies of the MRRs will be varied, which can be used to implement tunable fractional-order differentiation. In the experiment, a tunable fractional-order ranging from 0.57 to 2 has been successfully demonstrated.

2 Device fabrication and operation principle

An optical temporal differentiator provides the N-th order time derivative of the complex envelope of an input optical pulse [16]. The transfer function of an N-th order optical differentiator can be expressed as

$$H(\omega) = [\mathrm{j}(\omega - \omega_c)]^N, \quad (1)$$

where $\mathrm{j} = \sqrt{-1}$, ω and ω_c are the optical angular frequency and central angular frequency, respectively. It should be noted that N represents the differentiation order, which is not necessarily an integer, as a generalization of integer-order differentiation. An optical filter with a magnitude response of $|(\omega - \omega_c)|^N$ and a phase jump of $N\pi$ at ω_c, can be used to implement optical temporal differentiator.

Silicon based MRR is a promising scheme with advantages of compactness, well integration capability and compatibility with CMOS technology. As we know, an SOI MRR has a magnitude response of $|(\omega - \omega_c)|$ and a phase jump of π at the resonance frequency when the MRR meets in the condition of critical coupling. Thus the MRR can be used to implement first-order differentiation [12]. Moreover, when we apply direct current (DC) voltage source on the doped-silicon MRR and change the voltage, the magnitude and phase responses of the MRR vary simultaneously, and a tunable fractional-order differentiation can be implemented when the phase jump is not equal to π [23]. A detailed principle discussion can be referred in Ref. [23]. Therefore, to achieve a larger tunable order range, the electrically tuned MRR unit needs to be cascaded with all the resonance frequencies aligned.

Theoretically, an all-pass filter consisting of cascaded rings and a single bus waveguide is competent to the differentiation. However, for the convenience of experiments, we have designed three cascaded add-drop MRRs as shown in Fig. 1(a). There are two coupling bus waveguides to share these three rings. Despite of different design from all-pass filter, the principle of differentiation is the same. The cascaded MRRs are fabricated on the commercial SOI wafer. The top silicon thickness of the SOI wafer is 220 nm and the bottom buried oxide layer is 2 μm thick. To define the waveguide patterns, deep ultraviolet (DUV) photolithography using a 248 nm stepper was employed, followed by anisotropic dry etch of silicon. And boron and phosphorus ion implantations were performed to form the highly p-type and n-type doped regions. Also the slab layer was etched outside the p-i-n junctions to confine the current flow around the ring

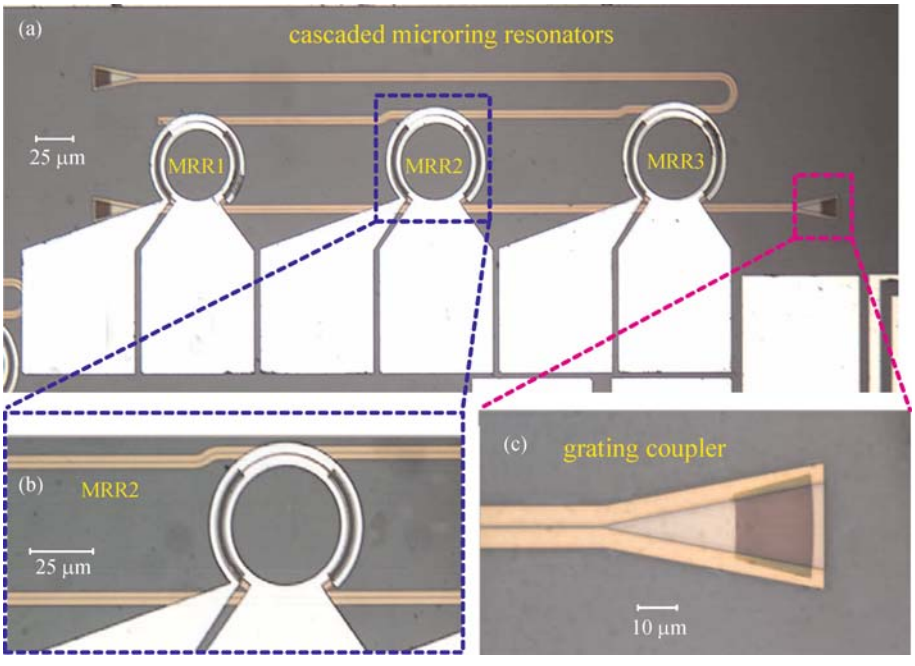

Fig. 1 (a)–(c) Microscope images of the cascaded MRRs, zoom-in ring region of MRR2 and zoom-in grating coupler, respectively

waveguide. Finally, contact holes were etched and aluminum was deposited to form the metal connection. Figures 1(a)–1(c) show the microscope images of the fabricated cascaded MRRs, the zoom-in ring region and grating coupler, respectively. All the waveguides widths are about 500 nm. The radii of the three MRRs are 54.44, 57.03, 59.88 μm, respectively. The trench width changes linearly from 180 to 340 nm and the etch depth is 70 nm. The coupling gap between the bus waveguide and bending waveguide is about 330 nm. And the period of the grating coupler is 610 nm and the period number is 35.

The measured transmission spectrum at the through port of the cascaded MRRs is illustrated in Fig. 2. And Fig. 2(b) shows the zoom-in region of two resonance wavelengths aligned. One can calculate from Fig. 2(a) that the corresponding free spectral ranges (FSRs) of the three MRRs are about 1.6, 1.688 and 1.8 nm, respectively. And the resonance wavelengths of MRR1 and MRR3 are overlapped at 1558.55 nm, which can be used to implement second-order differentiation. To achieve tunable fractional-order differentiation, we can apply three DC voltage sources on the cascaded three MRRs respectively. As the applied voltage on a single MRR (MRR1) increases, the loss of the ring waveguide increases, and the resonance frequency also experiences blue shift due to carrier dispersion effects, resulting in the magnitude and phase response changes, as shown in Figs. 3(a) and 3(b). When the voltage ranges from 0 to 1.0 V, a phase jump from π to 0.47π has been achieved. Further, when two DC voltage sources are used to provide different voltages applied on MRR1 and MRR3, some representative phase responses are as illustrated in Fig. 3(d) with phase jump of 1.2π, 1.5π,1.7π and 2π, respectively, and the corresponding magnitude responses are shown in Fig. 3(c). The biased voltage pairs are set at (0.95 V, 0.95 V), (0.8 V, 0.9 V), (0 V, 0.9 V), and (0 V, 0 V). In these cases, two resonance wavelengths of two MRRs are aligned. From Fig. 3 we can see that, the cascaded MRRs have potential to implement a tunable fractional-order differentiator with a tuning range of 0.47–2. However, when the MRR is biased with different voltages, the operation wavelength will be shifted due to carrier dispersion effects. To make sure that the operation wavelengths are identical, a possible solution is to use additional thermal tuning pads to stabilize the shift of wavelength caused by electrical tuning pads [25]. All these spectra are measured by an optical spectrum analyzer (OSA, AQ6370B) with a resolution of 0.02 nm, and phase responses are measured by a photonic dispersion and loss analyzer (Agilent, 86038B).

3 Experimental results

Figure 4 shows the schematic diagram for the proposed tunable fractional-order differentiator. A continuous wave (CW) is emitted by a tunable laser source (TLS) with a tuning resolution of 0.01 nm, which enables us to precisely align to the resonance wavelengths of the cascaded MRRs. And then the CW light is modulated by a Mach-Zehnder modulator (MZM) driven with a sinusoidal radio

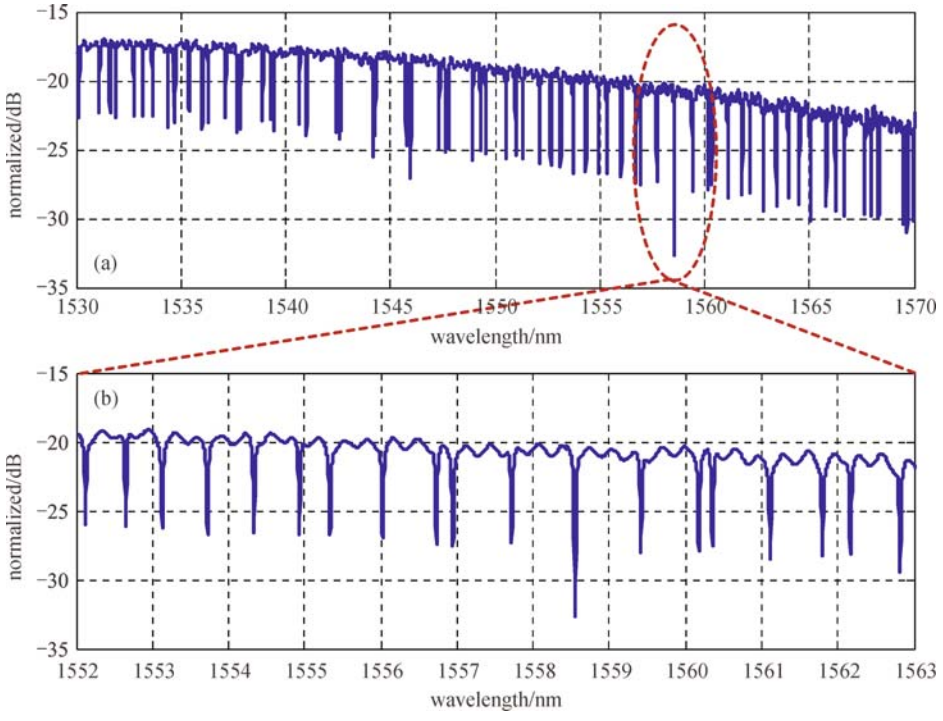

Fig. 2 (a) Measured transmission spectrum of the cascaded MRRs; (b) is the zoom-in region of two resonance wavelengths aligned

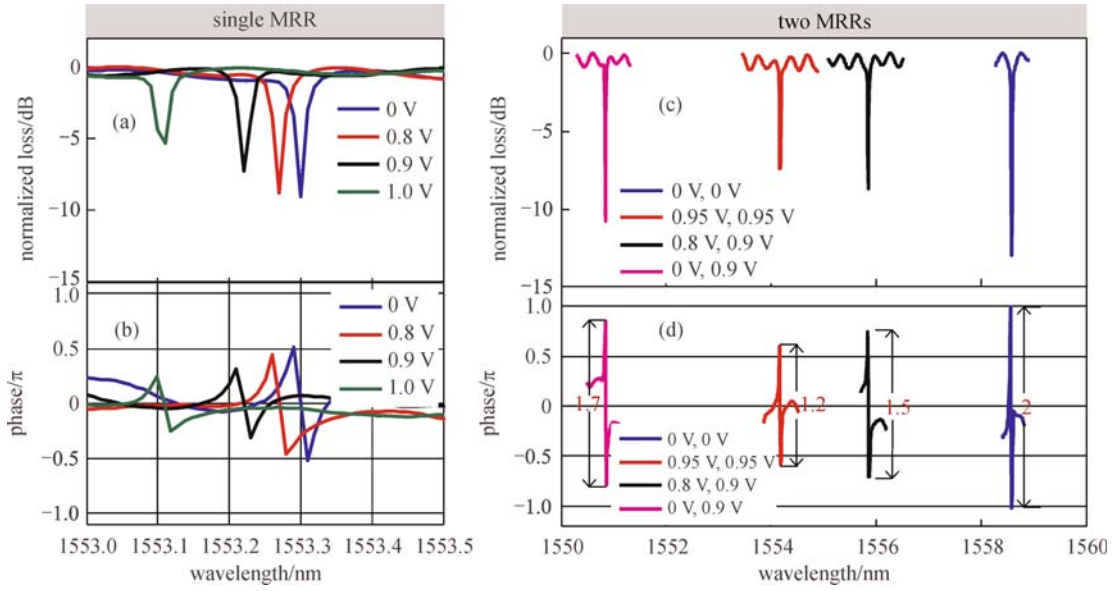

Fig. 3 (a) and (b) are the measured magnitude responses and phase responses with different voltages applied on a single MRR (MRR1), respectively. The biased voltages are set at 0, 0.8, 0.9, and 1.0 V. (c) and (d) are the measured magnitude responses and phase responses with different voltages applied on two MRRs (MRR1 and MRR3), respectively. The biased voltage pairs are set at (0.95 V, 0.95 V), (0.8 V, 0.9 V), (0 V, 0.9 V), and (0 V, 0 V). In these cases, two resonance wavelengths are aligned

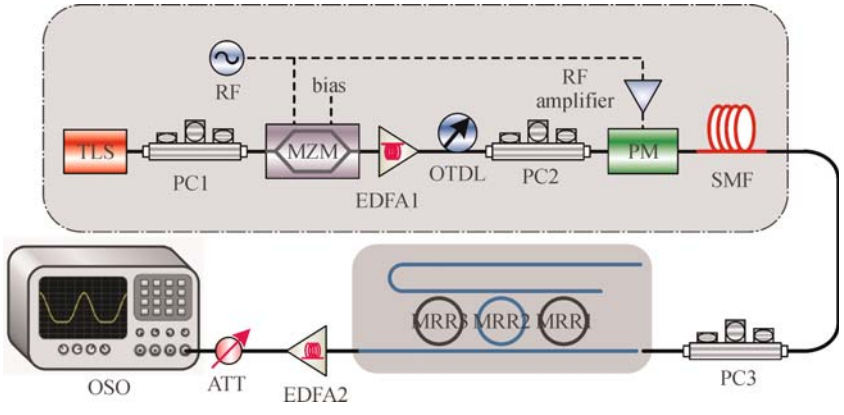

Fig. 4 Schematic diagram of the experimental setup

frequency (RF) clock signal with a fixed frequency of 10 GHz. To obtain a DC free pulse from the MZM, the driving parameters of the MZM should be carefully adjusted. Utilizing the nonlinear transmission curve of the MZM, a return-to-zero (RZ) pulse will be obtained when the DC bias of MZM is adjusted to below the quadrature point and the amplitude of RF signal is less than V_π. In this way, the pulse duty cycle can be less than 50%. Then the pulse passes through a phase modulation to induce chirp. The optical tunable delay line (OTDL) is used to adjust the alignment of the MZM and phase modulator (PM). Then a segment of single mode fiber (SMF) is used to compensate the chirp. It is known that as the SMF length increases, the full width at half-maximum (FWHM) is decreased to the minimum, and then is increased subsequently. To get a shortest pulse, we need to optimize the SMF length so that the pulse chirp can be totally compensated by the SMF dispersion [26]. In the experiment, by changing the input RF power along with the length of the SMF, pulses with different FWHMs can be obtained.

Subsequently, the generated optical signal is coupled into the cascaded MRRs using vertical grating coupling method. For the experimental restraints, only two DC voltage sources are used to provide different voltages applied on MRR1 and MRR3 respectively. Then the output signal at the through port of the cascaded MRRs is amplified by an erbium doped fiber amplifier (EDFA) to compensate the loss of the cascaded MRRs and finally recorded by an ultra-high optical sampling oscilloscope (OSO) (Alnair Laboratories, Eye-1000C) with 500-GHz

bandwidth and a temporal resolution of 1 ps. By changing the voltages applied on the MRRs and aligning the resonance wavelengths, we can observe different output waveforms, corresponding to different differentiation orders.

First, when we just employ MRR1 and apply one DC voltage source applied on it, we use a Gaussian input with a FWHM of 30 ps as shown in Fig. 5(a). By changing the voltage, the measured output waveforms (blue solid lines) are as shown in Figs. 6(a)–6(d), corresponding to different differentiation orders of 0.57, 0.71, 0.84 and 0.97 respectively, and the simulated waveforms for ideal fractional-order differentiation are for comparison (red dot lines). Figure 6(e) shows the spectra of the input Gaussian pulse (blue line) and the output waveform (red line) in the case of $N = 0.97$. It should be noted that we choose the resonance wavelength of 1553.27 nm when no biased voltage applied. To tune the fractional order of differentiation, the resonance wavelength is inevitably shifted slightly. Thus the input central wavelength will be adjusted properly. To accurately evaluate the errors of differentiation, we need to define a parameter of average deviation, which is defined as the mean absolute deviation of measured waveforms from the simulated ones on certain pulse period. The deviations are about 4.26%, 4.39%, 4.72% and 6.21%, respectively. One can see that the output waveforms agree well with the ideal simulated ones.

Then, we employ MRR1 and MRR3 and apply two DC voltage sources applied on them respectively. As we know, cascading of multi MRRs will lead to the reduce of the output energy efficiency, and it is an effective way to improve the energy efficiency by increasing the bandwidth of the input signal. So we use an input Gaussian pulse with FWHM of 18 ps, as depicted in Fig. 5(b). By changing the voltages simultaneously, the measured output waveforms (blue solid lines) are as shown in Figs. 7(a)–7(d), and the simulated waveforms for ideal fractional-order differentiation are for comparison (red dot lines). Figures 7(a)–7(d) correspond to the output waveforms with different differentiation orders of 1.55, 1.78, 1.94 and 2 respectively.

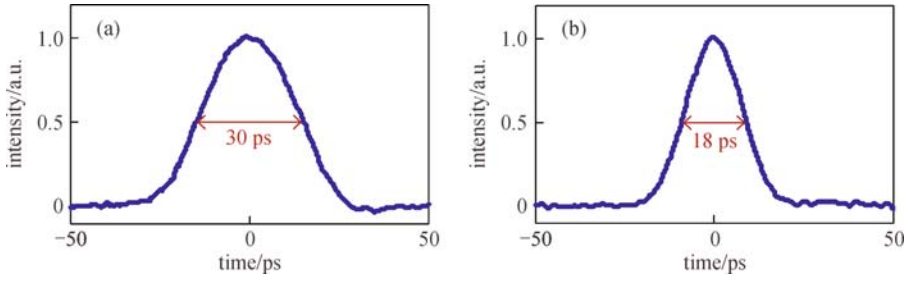

Fig. 5 Output waveforms of SMF with different FWHMs. (a) FWHM is 30 ps; (b) FWHM is 18 ps

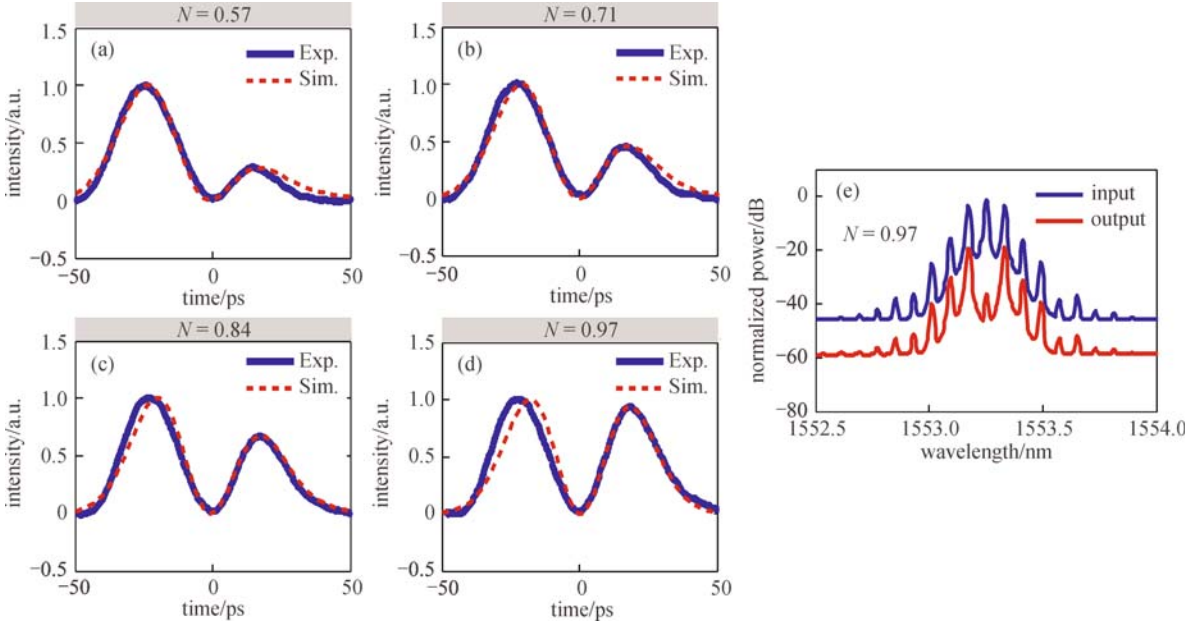

Fig. 6 Experimental results for MRR1. (a)–(d) are the output waveforms with different voltages applied on MRR1, corresponding to differentiation orders of 0.57, 0.71, 0.84 and 0.97 respectively. (e) is the spectra of input Gaussian pulse (blue line) and the output waveform (red line) when $N = 0.97$

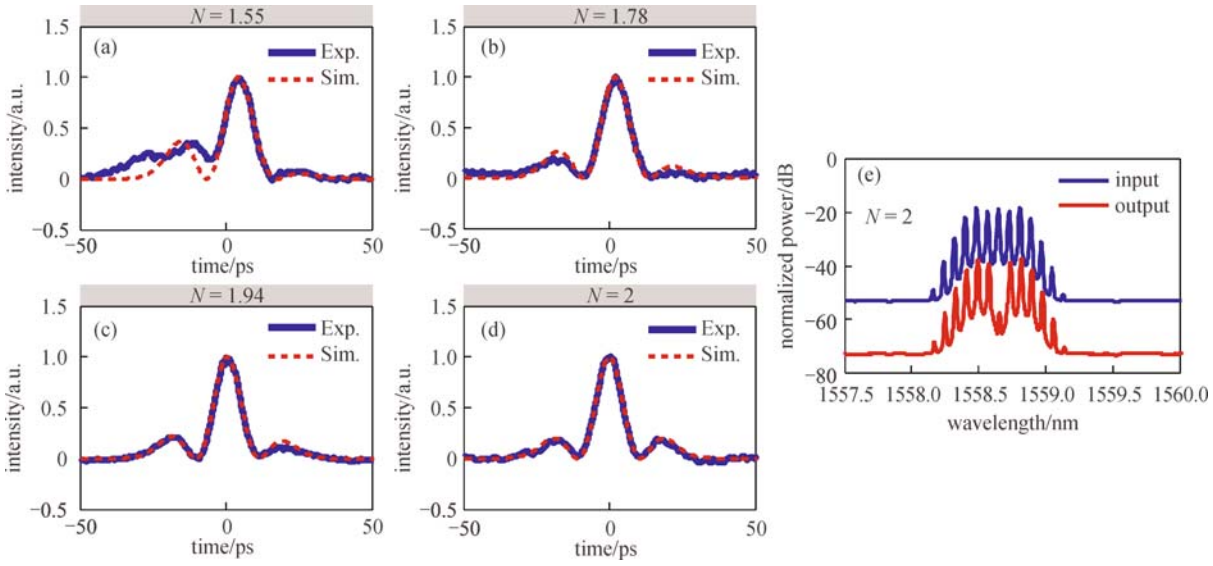

Fig. 7 Experimental results for cascaded MRR1 and MRR3. (a)–(d) are the output waveforms with different voltages applied on MRR1 and MRR3, corresponding to differentiation orders of 1.55, 1.78, 1.94 and 2 respectively. (e) is the spectra of input Gaussian pulse (blue line) and the output waveform (red line) when $N = 2$

Figure 7(e) shows the spectra of input Gaussian pulse (blue line) and the output waveform (red line) in the case of $N = 2$. And the corresponding calculated deviations are about 6.02%, 3.45%, 1.70% and 1.89%, respectively. One can see that the output waveforms also agree well with the ideal simulated ones. Thus, we have a tunable order range from 0.57 to 2, and all the experimental waveforms agree well with the simulated ones.

4 Conclusions

We have experimentally demonstrated an all-optical continuously tunable fractional-order differentiator using on-chip cascaded electrically tuned MRRs. The change of the voltage applied on the MRR leads to change of the waveguide propagation loss, resulting in the change of the phase shift of the MRR, which can be used to implement fractional-order differentiation. To achieve a larger tunable range, two DC voltage sources are applied on two cascaded MRRs, and a tunable order range from 0.57 to 2 has been demonstrated with Gaussian pulse injection. All the differentiation deviations are less than 7%.

Acknowledgements This work was partially supported by the National Basic Research Program of China (No. 2011CB301704), the Program for New Century Excellent Talents in Ministry of Education of China (No. NCET-11-0168), and the National Natural Science Foundation of China (Grant Nos. 11174096 and 61475052).

References

1. Azaña J, Madsen C, Takiguchi K, Cincotti G. Guest editorial optical signal processing. Journal of Lightwave Technology, 2006, 24(7): 2484–2486
2. Ngo N Q, Yu S F, Tjin S C, Kam C H. A new theoretical basis of higher-derivative optical differentiators. Optics Communications, 2004, 230(1–3): 115–129
3. Berger N K, Levit B, Fischer B, Kulishov M, Plant D V, Azaña J. Temporal differentiation of optical signals using a phase-shifted fiber Bragg grating. Optics Express, 2007, 15(2): 371–381
4. Liu F, Wang T, Qiang L, Ye T, Zhang Z, Qiu M, Su Y. Compact optical temporal differentiator based on silicon microring resonator. Optics Express, 2008, 16(20): 15880–15886
5. Slavík R, Park Y, Kulishov M, Morandotti R, Azaña J. Ultrafast all-optical differentiators. Optics Express, 2006, 14(22): 10699–10707
6. Kulishov M, Azaña J. Long-period fiber gratings as ultrafast optical differentiators. Optics Letters, 2005, 30(20): 2700–2702
7. Xu J, Zhang X, Dong J, Liu D, Huang D. High-speed all-optical differentiator based on a semiconductor optical amplifier and an optical filter. Optics Letters, 2007, 32(13): 1872–1874
8. Li M, Janner D, Yao J, Pruneri V. Arbitrary-order all-fiber temporal differentiator based on a fiber Bragg grating: design and experimental demonstration. Optics Express, 2009, 17(22): 19798–19807
9. Park Y, Azaña J, Slavík R. Ultrafast all-optical first- and higher-order differentiators based on interferometers. Optics Letters, 2007, 32(6): 710–712
10. Li Z, Wu C. All-optical differentiator and high-speed pulse generation based on cross-polarization modulation in a semiconductor optical amplifier. Optics Letters, 2009, 34(6): 830–832
11. Hu Y, Zhang L, Xiao X, Li Z, Li Y, Chu T, Su Y, Yu Y, Yu J. An ultra-high-speed photonic temporal differentiator using cascaded SOI microring resonators. Journal of Optics, 2012, 14(6): 065501
12. Dong J, Zheng A, Gao D, Liao S, Lei L, Huang D, Zhang X. High-order photonic differentiator employing on-chip cascaded microring resonators. Optics Letters, 2013, 38(5): 628–630

13. Dong J, Zheng A, Gao D, Lei L, Huang D, Zhang X. Compact, flexible and versatile photonic differentiator using silicon Mach-Zehnder interferometers. Optics Express, 2013, 21(6): 7014–7024
14. Li M, Jeong H S, Azaña J, Ahn T J. 25-terahertz-bandwidth all-optical temporal differentiator. Optics Express, 2012, 20(27): 28273–28280
15. Ahn T J, Azaña J. Wavelength-selective directional couplers as ultrafast optical differentiators. Optics Express, 2011, 19(8): 7625–7632
16. Cuadrado-Laborde C. All-optical ultrafast fractional differentiator. Optical and Quantum Electronics, 2008, 40(13): 983–990
17. Cuadrado-Laborde C, Andrés M V. In-fiber all-optical fractional differentiator. Optics Letters, 2009, 34(6): 833–835
18. Cuadrado-Laborde C, Andrés M V. Design of an ultra-broadband all-optical fractional differentiator with a long-period fiber grating. Optical and Quantum Electronics, 2011, 42(9–10): 571–576
19. Li M, Shao L Y, Albert J, Yao J P. Continuously tunable photonic fractional temporal differentiator based on a tilted fiber Bragg grating. IEEE Photonics Technology Letters, 2011, 23(4): 251–253
20. Shahoei H, Albert J, Yao J P. Tunable fractional order temporal differentiator by optically pumping a tilted fiber Bragg grating. IEEE Photonics Technology Letters, 2012, 24(9): 730–732
21. Shahoei H, Xu D X, Schmid J H, Yao J P. Photonic fractional-order differentiator using an SOI microring resonator with an MMI coupler. IEEE Photonics Technology Letters, 2013, 25(15): 1408–1411
22. Zheng A, Yang T, Xiao X, Yang Q, Zhang X, Dong J. Tunable fractional-order differentiator using an electrically tuned silicon-on-isolator Mach-Zehnder interferometer. Optics Express, 2014, 22 (15): 18232–18237
23. Zheng A, Dong J, Zhou L, Xiao X, Yang Q, Zhang X, Chen J. Fractional-order photonic differentiator using an on-chip microring resonator. Optics Letters, 2014, 39(21): 6355–6358
24. Jin B, Yuan J, Yu C, Sang X, Wu Q, Li F, Wang K, Yan B, Farrell G, Wai P K A. Tunable fractional-order photonic differentiator based on the inverse Raman scattering in a silicon microring resonator. Optics Express, 2015, 23(9): 11141–11151
25. Qiu Y, Xiao X, Luo M, Li C, Yang Q, Yu S. Tunable, narrow linewidth silicon micro-ring laser source for coherent optical communications. In: Proceedings of CLEO:QELS_Fundamental Science. San Jose, California: Optical Society of America, 2015, JTh2A.57
26. Yang T, Dong J, Liao S, Huang D, Zhang X. Comparison analysis of optical frequency comb generation with nonlinear effects in highly nonlinear fibers. Optics Express, 2013, 21(7): 8508–8520

Jianji Dong is professor in Wuhan National Laboratory for Optoelectronics, Huazhong University of Science and Technology (HUST), Wuhan, China. He is working on the silicon photonics, photonic computing, and microwave photonics. He is an Editorial Board Member of *Scientific Reports*. He received the National Best Dissertations Award in 2010 and the first award of Natural Science of Hubei Province in 2013.